

Asymmetric Dimers Can Be Formed by Dewetting Half-Shells of Gold Deposited on the Surfaces of Spherical Oxide Colloids

Yu Lu,[†] Hui Xiong,[†] Xuchuan Jiang, and Younan Xia*

Department of Chemistry, Department of Materials Science and Engineering, University of Washington, Seattle, Washington 98195

Mara Prentiss[§] and George M. Whitesides[‡]

Department of Physics, Department of Chemistry and Chemical Biology, Harvard University, Cambridge, Massachusetts 02138

Received July 15, 2003; E-mail: xia@chem.washington.edu

The availability of spherical colloids that are uniform in size, composition, and surface charge has played an important role in elucidating the optical, rheological, and electrokinetic properties characteristic of colloidal materials.¹ Spherical colloids have also been exploited as building blocks to generate three-dimensionally periodic lattices (e.g., colloidal crystals, opals, and inverse opals) through self-assembly.² To this end, these structures have been explored as a unique system to generate photonic band gaps that are useful in controlling the propagation of electromagnetic waves in three dimensions of space.³

Despite their predominant role in colloid science, spherical colloids are not necessarily the best candidate for all studies on colloids. For example, computational studies have indicated that they are not well-suited for use as building blocks in generating photonic crystals with complete band gaps due to the degeneracy caused by the spherical symmetry of lattice points.⁴ Nonspherical particles may offer some immediate advantages over the spherical counterparts in applications that require colloidal systems with higher complexities and crystalline lattices of lower symmetries. Among all approaches to nonspherical colloids, those capable of generating truly monodispersed samples were all based on the modification of monodispersed spherical colloids.⁵ For example, by mechanically stretching spherical colloids embedded in polymeric matrices, it was possible to obtain ellipsoidal beads as monodispersed samples.⁶ By swelling polymer beads with a monomer, followed by polymerization and phase-separation, it was possible to form pearl- or peanut-shaped colloidal particles.⁷ By depositing thin films of an additional material onto spherical colloids as half-shells, it was possible to produce colloidal beads patterned with regions of different properties.⁸ It has also been demonstrated that spherical colloids could be assembled into polygonal/polyhedral aggregates under the physical confinement provided by various templates.⁹ Here we describe another method (Figure S1) that generates asymmetric dimers of gold microcrystals and spherical oxide colloids by depositing a thin film of gold onto the spherical colloids, followed by thermal annealing.

Figure 1A shows the SEM image of an array of 600-nm silica beads prepared by placing a drop of the aqueous suspension on a silicon wafer, followed by evaporation under ambient conditions. An adhesion layer of Ti/W alloy was first deposited onto these silica beads using a sputter, followed by another thin layer of gold. According to previous work, these thin layers of metals formed half-shells on top of each spherical colloid.¹⁰ Figure 1B shows an SEM image of this sample after it had been placed in an oven. As

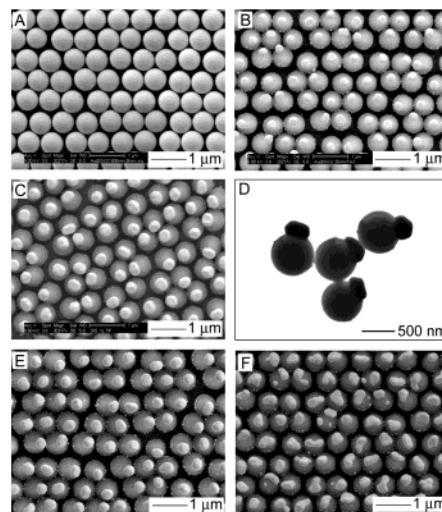


Figure 1. (A) SEM image of an array of 600-nm silica beads whose surfaces had been coated with two layers of half-shell consisting of Ti/W alloy (5 nm thick) and gold (25 nm thick). (B) SEM image of this array after it had been annealed in air at 700 °C for 3 h. The gold half-shell had dewetted to form a microcrystal on top of each individual silica bead. (C) SEM image of another array of 600-nm silica beads whose surfaces were decorated with gold microcrystals of ~320 nm in size that resulted from the dewetting of gold half-shells of 40 nm thick. (D) TEM image of several Au/SiO₂ dimers shown in (C), after they had been released by sonication and then redeposited on a carbon-coated copper grid. (E, F) SEM images of two other samples where the silica beads (600 nm in diameter) were coated with half-shells of Ti/W alloy (5 nm thick) and gold (25 nm thick), followed by annealing at 700 °C for 3 h in an environment of Ar and H₂, respectively.

the sample was annealed, the mobility of gold atoms was greatly increased, and each gold half-shell beaded up by dewetting from its edge where it was the thinnest.¹¹ Each gold half-shell was then transformed into a microcrystal sitting atop of the silica bead. The gold microcrystals formed via this process were relatively uniform in shape and size, with their dimensions close to ~250 nm. When silica beads of the same size were used, the sizes of gold microcrystals could be controlled by varying the thickness of gold half-shells. Figure 1C shows the SEM image of another sample where the silica beads were also 600 nm in diameter, but the thickness of gold half-shells had been increased from 25 to 40 nm. In consequence, the lateral dimensions of resultant gold microcrystals were increased from ~250 to ~340 nm. Figure 1D shows a TEM image of free-standing Au/SiO₂ dimers that had been released from the substrate through a brief sonication. It is obvious that the silica beads maintained their spherical shape in this

[†] Department of Materials Science and Engineering, University of Washington.

[§] Department of Physics, Harvard University.

[‡] Department of Chemistry and Chemical Biology, Harvard University.

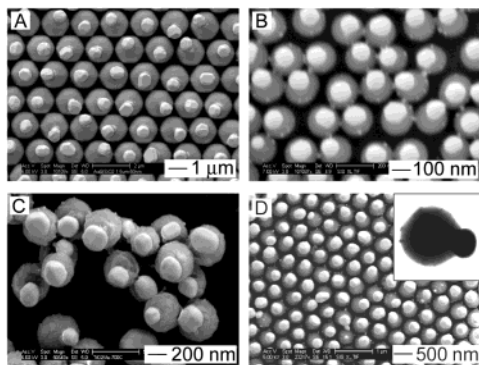


Figure 2. (A) SEM image of an array of 1.5- μm silica beads whose surfaces were decorated with gold crystals of ~ 650 nm in size. These crystals resulted from gold half-shells of 40 nm thick. (B) SEM image of an array of 200-nm silica beads whose surfaces were capped with gold crystals of ~ 100 nm in size that evolved from gold half-shells of 13 nm thick. (C) SEM image of 400-nm anatase spheres capped with gold crystals of ~ 250 nm in size that derived from gold half-shells of 26 nm thick. (D) SEM image of dimers containing magnetic spherical colloids and gold microcrystals of ~ 300 nm in size. The samples shown in (A–C) were annealed in air at 700 $^{\circ}\text{C}$ for 3 h, and the sample.

annealing process. Both SEM and TEM images indicate the formation of well-defined facets for each gold microcrystal, and a good adhesion between the gold microcrystal and corresponding silica bead. The appearance of well-defined facets suggests that each gold microcrystal was highly crystalline (Figure S2). Parts E and F of Figure 1 show SEM images of two additional samples that were prepared using a procedure similar to that used for Figure 1B, except that the gas had been switched from air to Ar and H_2 , respectively. For these two samples, the use of Ar did not cause obvious change in morphology and dimensions for the resultant gold microcrystals, but the use of H_2 led to the formation of gold microcrystals with poorly defined shapes and nonuniform sizes. It is believed that these differences were probably caused by the change in surface energy, one of the major driving forces for gold dewetting, when the annealing environment was changed from air or Ar to H_2 . Similar effects have also been observed when metal islands deposited on a flat surface were annealed at an elevated temperature.¹²

This procedure could be readily extended to silica beads with diameters other than 600 nm. Figure 2A shows the SEM image of an array of asymmetric dimers that were prepared with silica beads of 1.5 μm in diameter. The gold half-shells were 40 nm in thickness, and the resultant gold microcrystals were ~ 650 nm in size. Figure 2B shows the SEM image of another sample where the silica beads were 200 nm in diameter, and the gold half-shells, of 13 nm in thickness. For this sample, the gold microcrystals resulting from the dewetting process were measured at ~ 100 nm, representing the smallest size we have ever achieved. The current procedure is best suited for use with silica beads larger than ~ 200 nm, because smaller colloidal particles tend to deform viscoelastically at an elevated temperature.¹³ There was also an upper limit for the size of silica beads that could be successfully used with the current procedure, and this limit was around 2 μm . When silica colloids larger than 2 μm were employed, the gold half-shell tended to break into several small pieces on top of each silica bead upon heating. As a result, the surface of each individual silica bead was spatially decorated with more than one gold microcrystal.

Spherical colloids made of oxides other than silica have also been incorporated into the present procedure. Figure 2C shows the SEM image of asymmetric dimers fabricated from spherical colloids

made of anatase.¹⁴ In this case, the gold film was 26 nm thick. Figure 2D shows the SEM image of an additional sample, where the spherical colloids were obtained by coating polystyrene beads (loaded with magnetite nanoparticles) with silica shells. The gold film was 26 nm thick, and the sample was annealed at 700 $^{\circ}\text{C}$ for 3 h under Ar protection. In this case, the polystyrene was converted to carbon, and the magnetite nanoparticles were still responsive to an external magnetic field. We believe that the availability of such asymmetric dimers might enable one to easily manipulate the spatial position of bioactive molecules attached to the surfaces of gold microcrystals using a magnetic field. By controlling the size of the gold microcrystal, it should be possible to limit the number of molecules immobilized on the surface of each dimeric particle. In addition, it is believed that this method can be extended to cover metals other than gold, and ceramic oxides other than those described in this paper.

Acknowledgment. This research has been supported in part by a DARPA-DURINT subcontract from Harvard University and a David and Lucile Packard Fellowship. Y.X. is a Camille Dreyfus Teacher Scholar. Y.L. thanks the Center for Nanotechnology at the UW for the Nanotech Fellowship Award.

Supporting Information Available: Experimental procedure, as well as EDX spectrum and XRD pattern of the gold microcrystals (PDF). This material is available free of charge via the Internet at <http://pubs.acs.org>.

References

- (1) See, for example: (a) Matijevic, E. *Langmuir* **1994**, *10*, 8. (b) Xia, Y.; Gates, B.; Yin, Y.; Lu, Y. *Adv. Mater.* **2000**, *12*, 693. (c) Dinsmore, A. D.; Crocker, J. C.; Yodh, A. G. *Curr. Opin. Colloid Interface Sci.* **1998**, *3*, 5.
- (2) (a) Pieranski, P. *Contemp. Phys.* **1983**, *24*, 25. (b) Murray, C. A.; Grier, D. G. *Am. Sci.* **1995**, *83*, 238. (c) Gast, A. P.; Russel, W. B. *Phys. Today* **1998**, *December*, 24.
- (3) Recent reviews: (a) Grier, D. G. From Dynamics to Devices: Directed Self-Assembly of Colloidal Materials, a special issue in *MRS Bull.* **1998**, *23*, 21. (b) Polman, A.; Wiltzius, P. Materials Science Aspects of Photonic Crystals, a special issue in *MRS Bull.* **2001**, *26*, 608. (c) Velev, O. D.; Lenhoff, A. M. *Curr. Opin. Colloid Interface Sci.* **2000**, *5*, 56. (d) Stein, A.; Schroden, R. C. *Curr. Opin. Solid State Mater. Sci.* **2001**, *5*, 553. (f) Xia, Y. Photonic Crystals, a special issue in *Adv. Mater.* **2001**, *13*, 369.
- (4) Li, Z. Y.; Wang, J.; Gu, B. Y. *J. Phys. Soc. Jpn.* **1998**, *67*, 3288.
- (5) See, for example: Lu, Y.; Yin, Y.; Xia, Y. *Adv. Mater.* **2001**, *13*, 415.
- (6) (a) Sutura, S. P.; Boylan, C. W. *J. Colloid Interface Sci.* **1980**, *73*, 29. (b) Nagy, M.; Keller, A. *Polymer Comm.* **1989**, *30*, 130. (c) Keville, K. M.; Franses, E. I.; Caruthers, J. M. *J. Colloid Interface Sci.* **1991**, *144*, 103. (d) Jiang, P.; Bertone, J. F.; Colvin, V. L. *Science* **2001**, *291*, 453. (e) Lu, Y.; Yin, Y.; Xia, Y. *Adv. Mater.* **2001**, *13*, 271.
- (7) (a) Skjeltop, A. T.; Ugelstad, J.; Ellingsen, T. *J. Colloid Interface Sci.* **1996**, *113*, 577. (b) Sheu, H. R.; El-Aasser, M. S.; Vanderhoff, J. W. *Polym. Mater. Sci. Eng.* **1988**, *59*, 1185. (c) Okubo, M.; Yamashita, T.; Suzuki, T.; Shimizu, T. *Colloid Polym. Sci.* **1997**, *275*, 288.
- (8) (a) Takei, H.; Shimizu, N. *Langmuir* **1997**, *13*, 1865. (b) Petit, L.; Sellier, E.; Dugué, E.; Ravaine, S.; Mingotaud, C. *J. Mater. Chem.* **2000**, *10*, 253. (c) Alexander, C.; Vulfsen, E. N. *Adv. Mater.* **1997**, *9*, 751. (d) Bao, Z.; Chen, L.; Weldon, M.; Chandross, E.; Cherniavskaya, O.; Dai, Y.; Tok, J. B.-H. *Chem. Mater.* **2002**, *14*, 24. (e) Choi, J.; Zhao, Y.; Zhang, D.; Lo, Y. H. *Nano Lett.* **2003**, *3*, 995.
- (9) (a) Yin, Y.; Lu, Y.; Gates, B.; Xia, Y. *J. Am. Chem. Soc.* **2001**, *123*, 8718. (b) Yin, Y.; Xia, Y. *Adv. Mater.* **2001**, *13*, 267. (c) Aizenberg, J.; Braun, P. V.; Wiltzius, P. *Phys. Rev. Lett.* **2000**, *84*, 2997. (d) Velev, O. D.; Lenhoff, A. M.; Kaler, E. W. *Science* **2000**, *287*, 2240. (e) Zheng, H.; Lee, I.; Rubner, M. F.; Hammond, P. T. *Adv. Mater.* **2002**, *14*, 569. (f) Novak, J. P.; Nickerson, C.; Franzen, S.; Feldheim, D. L. *Anal. Chem.* **2001**, *73*, 5758. (g) Ozin, G. A.; Yang, M. Y. *Adv. Func. Mater.* **2001**, *11*, 95.
- (10) Love, J. C.; Gates, B. D.; Wolfe, D. B.; Paul, K. E.; Whitesides, G. M. *Nano Lett.* **2002**, *2*, 891.
- (11) Robinson, I. K.; Vartanyants, I. A.; Williams, G. J.; Pfeifer, M. A.; Pitney, J. A. *Phys. Rev. Lett.* **2001**, *87*, 195505.
- (12) Venables, J. A. *Introduction to Surface and Thin Film Processes*; Cambridge University Press: Cambridge, UK, 2000.
- (13) Mazur, S.; Beckerbauer, R.; Buckholz, J. *Langmuir* **1997**, *13*, 4287.
- (14) Jiang, X.; Herricks, T.; Xia, Y. *Adv. Mater.* **2003**, *15*, 1205.

JA0373014